

# Remote plasma etching of silicon nitride and silicon dioxide using $\text{NF}_3/\text{O}_2$ gas mixtures

B. E. E. Kastenmeier,<sup>a)</sup> P. J. Matsuo, and G. S. Oehrlein<sup>b)</sup>

*Department of Physics, The University at Albany, State University of New York, Albany, New York 12222*

J. G. Langan

*Air Products and Chemicals, Inc., Allentown, Pennsylvania 18195*

(Received 8 May 1997; accepted 2 January 1998)

The etching of silicon nitride ( $\text{Si}_3\text{N}_4$ ) and silicon dioxide ( $\text{SiO}_2$ ) in the afterglow of  $\text{NF}_3$  and  $\text{NF}_3/\text{O}_2$  microwave discharges has been characterized. The etch rates of both materials increase approximately linearly with the flow of  $\text{NF}_3$  due to the increased availability of F atoms. The etch rate of  $\text{Si}_3\text{N}_4$  is enhanced significantly upon  $\text{O}_2$  injection into the  $\text{NF}_3$  discharge for  $\text{O}_2/\text{NF}_3$  ratios of 0.3 and higher, whereas the  $\text{SiO}_2$  etch rate is less influenced for the same flow ratios. X-ray photoelectron spectroscopy of processed  $\text{Si}_3\text{N}_4$  samples shows that the fluorine content of the reactive layer, which forms on the  $\text{Si}_3\text{N}_4$  surface during etching, decreases with the flow of  $\text{O}_2$ , and instead oxidation and nitrogen depletion of the surface occur. The oxidation of the reactive layer follows the same dependence on the flow of  $\text{O}_2$  as the etch rate. Argon actinometry and quadrupole mass spectrometry are used to identify reactive species in the etching of both materials. The atomic fluorine density decreases due to dilution as  $\text{O}_2$  is added to the discharge. The mass spectrometer did not detect  $\text{NF}_x$  species ( $x=1-3$ ) at any discharge parameter setting, which indicates the near complete dissociation of  $\text{NF}_3$ . Nitric oxide (NO) was detected by mass spectrometry, and the NO density shows the same dependence on  $\text{O}_2$  flow as the  $\text{Si}_3\text{N}_4$  etch rate and the surface oxidation. Based on this observation, we propose that the etch rate enhancement for  $\text{Si}_3\text{N}_4$  is due to the adsorption of the NO on the  $\text{Si}_3\text{N}_4$  surface, followed by the formation of  $\text{N}_2$  with a N atom from the surface. The O atom can then attach to the same surface site, contributing to the oxidation. © 1998 American Vacuum Society. [S0734-2101(98)00604-6]

## I. INTRODUCTION

The minimization of feature sizes forces the semiconductor industry to constantly improve fabrication processes. For example, ion induced damage to oxide layers is not acceptable as the gate oxide thickness approaches 50 Å or less. Therefore, mask materials are increasingly stripped downstream from a remote plasma source, avoiding the bombardment of the surface with energetic ions, which is typical for a direct plasma process. Also, reactors for chemical vapor deposition need to be cleaned periodically in order to ensure a constant high quality of the thin films deposited.<sup>1</sup> Currently, plasma enhanced chemical vapor deposition (PECVD) chambers are often cleaned *in situ*, which can result in damage to chamber parts because of the presence of both fluorine and ion bombardment on electrodes. Low-pressure chemical vapor deposition (LPCVD) tubes are cleaned using a wet chemistry, e.g., hydrofluoric acid for the cleaning of LPCVD Si and  $\text{Si}_3\text{N}_4$  tubes.

A procedure that minimizes tool downtime and chamber damage, avoids the disposal of wet chemicals, and potentially enables a higher level of cleanliness, is remote plasma cleaning. The reactive afterglow of etching gases can be used to strip deposited layers off reactor walls and to clean the

chamber. This method is applicable in CVD reactors for Si,  $\text{SiO}_2$ ,  $\text{Si}_3\text{N}_4$ , and tungsten compounds.<sup>1-3</sup>

The etching characteristics of fluorocarbon gases like  $\text{CF}_4$  and  $\text{C}_2\text{F}_6$  have been widely studied. These gases are used for reactor cleaning, but since etching often occurs together with the formation of an undesired fluorocarbon polymer layer, they require the addition of  $\text{O}_2$ . A clean alternative to those gases is nitrogen trifluoride,  $\text{NF}_3$ , and mixtures of  $\text{NF}_3$  with  $\text{O}_2$ . Discharges of  $\text{NF}_3$  are not polymerizing, and thus a good choice for cleaning applications. Nitrogen trifluoride is environmentally preferable to  $\text{CF}_4$  and  $\text{C}_2\text{F}_6$  because it has a shorter atmospheric lifetime.<sup>4</sup> Another advantage of  $\text{NF}_3$  over fluorocarbon gases is that the dissociation of  $\text{NF}_3$  in a discharge can approach 100%, resulting in higher F atom concentrations and higher etch yields as compared to fluorocarbon gases.

In previous publications<sup>5-7</sup> the etching of  $\text{Si}_3\text{N}_4$  and  $\text{SiO}_2$  in remote  $\text{CF}_4$  discharges with  $\text{O}_2$  and  $\text{N}_2$  additions has been examined. It was found that the etch rate of  $\text{Si}_3\text{N}_4$  is strongly enhanced when both  $\text{O}_2$  and  $\text{N}_2$  are added to the  $\text{CF}_4$  discharge, but the  $\text{SiO}_2$  etch rate remains unchanged. A linear correlation between the  $\text{Si}_3\text{N}_4$  etch rate and the density of NO was observed,<sup>5,7</sup> and Blain *et al.*<sup>6</sup> suggested three models for the chemical effect of the NO on the nitride surface, all incorporating enhanced removal of the nitrogen. Surface effects of the NO molecule could also be observed for silicon etching.<sup>8</sup> The thickness of the reactive layer that forms on the

<sup>a)</sup>Electronic mail: bk7752@csc.albany.edu

<sup>b)</sup>Electronic mail: oehrlein@esilink.albany.edu

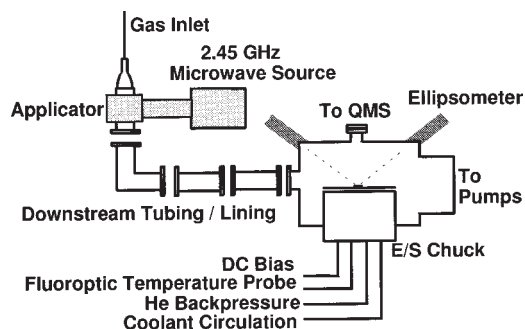


FIG. 1. Schematic of the chemical downstream etcher used in this investigation. The gases are fed into the sapphire applicator, where a microwave discharge is ignited. The species effluent from the plasma travel through tubing of variable length and lining material to the reactive chamber. The sample is placed on the center of an electrostatic chuck. A quadrupole mass spectrometer is mounted on the chamber on top of the sample, and monochromatic ellipsometry is used to determine etch rates.

crystalline Si during etching is reduced when NO is present, leading to an enhanced etch rate.

This article characterizes the etching of  $\text{Si}_3\text{N}_4$  and  $\text{SiO}_2$  in the afterglow of  $\text{NF}_3/\text{O}_2$  microwave discharges. Etch rates are reported as a function of  $\text{NF}_3$  flow and gas composition, and the reported etch rates are explained by the generation rate of active species, determined by optical emission actinometry and mass spectrometry. Furthermore, the etching mechanism of  $\text{Si}_3\text{N}_4$  in the presence of fluorine and NO in the gas phase is investigated in more detail by angular resolved x-ray photoelectron spectroscopy (XPS). Another article<sup>9</sup> will characterize the etching of polycrystalline Si in  $\text{NF}_3/\text{O}_2$  mixtures.

## II. EXPERIMENT

Figure 1 shows a schematic of the apparatus used for the experiments. Nitrogen trifluoride and mixtures of  $\text{NF}_3$  and  $\text{O}_2$  are excited using an Astex 2.45 GHz microwave applicator with a sapphire coupling tube. The pressure for all experiments was 1000 mTorr. The microwave power was varied from 600 to 1400 W, the flow of  $\text{NF}_3$  from 50 to 500 sccm. All experiments involving  $\text{O}_2$  were conducted at a microwave power level of 1400 W, with a constant flow of  $\text{NF}_3$  of either 300 or 500 sccm. A fiberoptic cable for optical emission experiments of the discharge is mounted on the housing of the applicator. The spectrograph used in this investigation is a 30 cm optical multichannel analyzer (EG&G PAR Model 1470) which covers the spectrum between 250 and 850 nm. The species produced in the plasma travel through a transport tube to the cylindrical reaction chamber. The length, geometry, and lining material of the transport tube can be varied. Samples of size 1 in.  $\times$  1 in. are glued on a 5 in. carrier wafer, which is placed on an electrostatic chuck in the reaction chamber. The materials used for this investigation are LPCVD  $\text{Si}_3\text{N}_4$  and thermally grown  $\text{SiO}_2$ . The temperature of the sample is monitored with a fluoroptic probe which contacts the backside of the sample. It was kept constant at 10 °C for all experiments. A pressure of 5 Torr of helium was maintained between the surface of the electro-

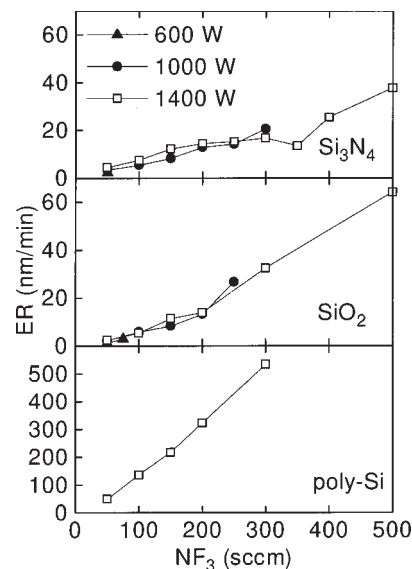


FIG. 2. The etch rate of  $\text{Si}_3\text{N}_4$ ,  $\text{SiO}_2$ , and polycrystalline silicon as a function of the flow of  $\text{NF}_3$ . The measurements were performed at a constant pressure of 1000 mTorr and with three different microwave power leads. The etch rate roughly increases linearly with the flow due to the increasing availability of reactive species.

static chuck and the carrier wafer in order to obtain good heat conduction. Etch rates are measured *in situ* by monochromatic ellipsometry (wavelength 632.8 nm). A quadrupole mass spectrometer (Leybold Inficon Transpector) is mounted on top of the reaction chamber such that the distance from the orifice to the discharge is the same as that from the sample to the discharge. The ionization region of the mass spectrometer is in line of sight with the sampling orifice and the reaction chamber. The energy of the ionizing electrons is 35 eV. The pressure in the mass spectrometer during an experiment is around  $1 \times 10^{-6}$  Torr. The reaction chamber is connected to an ultrahigh vacuum (UHV) wafer handling system which allows the samples to be moved to a multi-technique surface analysis chamber without exposure to air.

## III. RESULTS

### A. Etch rates

The etch rates of  $\text{Si}_3\text{N}_4$  and  $\text{SiO}_2$  were measured as a function of the flow of  $\text{NF}_3$  (see Fig. 2). The pressure was kept constant at 1000 mTorr, and the parameter for the curves in Fig. 2 is the microwave power. The flow range in which it was possible to obtain stable discharges depended on the power. At 600 W, for example, a stable discharge could be obtained only for 50 sccm of  $\text{NF}_3$ , whereas at 1400 W the flow of  $\text{NF}_3$  could be varied across the whole range permitted by the mass flow controller. The etch rates of all three materials increase linearly with the flow of  $\text{NF}_3$ . Since all curves coincide, microwave power does not influence the etch rate significantly. The  $\text{SiO}_2$  etch rates, however, grow faster with the flow of  $\text{NF}_3$  than the corresponding  $\text{Si}_3\text{N}_4$  etch rates, their slopes being greater by a factor of more than 2.

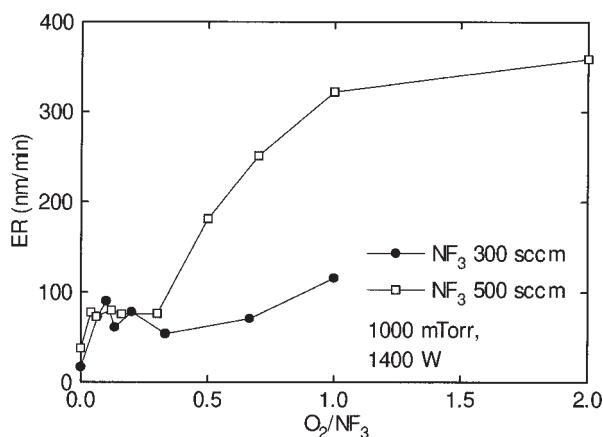


FIG. 3. The etch rate of silicon nitride vs the flow ratio of  $\text{O}_2$  and  $\text{NF}_3$ . The effect of oxygen addition is most pronounced for a high flow of  $\text{NF}_3$  (500 sccm).

The etch rate of polycrystalline Si is proportional to the density of atomic F if no significant oxidation of the silicon surface occurs.<sup>8,10</sup> Therefore, the F density can be calculated from the Si etch rate and published rate constants.<sup>11</sup> The etch rate of polycrystalline silicon is shown on the bottom panel of Fig. 2. It is also proportional to the  $\text{NF}_3$  flow, and higher than the  $\text{Si}_3\text{N}_4$  etch rate by a factor of 30. This comparison shows that F atoms, the primary etchants for Si and  $\text{Si}_3\text{N}_4$ , are available in abundance to sustain the etching of  $\text{Si}_3\text{N}_4$ , and that the etch rate of  $\text{Si}_3\text{N}_4$  is not limited by the density of atomic F.

Oxygen addition to a  $\text{NF}_3$  discharge strongly enhances the  $\text{Si}_3\text{N}_4$  etch rates. Figure 3 shows the etch rates of  $\text{Si}_3\text{N}_4$  as a function of the ratio  $\text{O}_2/\text{NF}_3$ . Pressure and microwave power were kept constant at 1000 mTorr and 1400 W, respectively. The flow of  $\text{NF}_3$  was fixed at either 300 or 500 sccm. A small amount of oxygen increases the etch rate by a factor of 2 for a  $\text{NF}_3$  flow of 500 sccm, and by a factor of 4.3 in the case of 300 sccm of  $\text{NF}_3$ . As the flow of  $\text{O}_2$  is increased further (up to  $\text{O}_2/\text{NF}_3=0.3$ ), the etch rates remain constant, and etch rates for 300 and 500 sccm of  $\text{NF}_3$  are identical. A significant difference is observed for high flows of oxygen ( $\text{O}_2/\text{NF}_3>0.3$ ). The etch rate for the low flow of  $\text{NF}_3$  remains on the same low level, whereas the etch rate for the high  $\text{NF}_3$  flow increases continuously until it saturates near  $\text{O}_2/\text{NF}_3=1$ .

Oxygen addition to a discharge of 300 or 500 sccm of  $\text{NF}_3$  does not affect the silicon dioxide etch rates as strongly as it does the silicon nitride etch rates. Figure 4 shows the etch rates of  $\text{SiO}_2$  for ratios  $\text{O}_2/\text{NF}_3=0$  to 1. In the case of 500 sccm of  $\text{NF}_3$ , the etch rate remains almost constant up to ratios  $\text{O}_2/\text{NF}_3=0.5$ , and then increases slightly. If oxygen is added to a lower flow of  $\text{NF}_3$  (300 sccm), the etch rate of  $\text{SiO}_2$  actually decreases.

For certain unstable plasma conditions, etch rates of  $\text{Si}_3\text{N}_4$  and  $\text{SiO}_2$  were found to be abnormally high. These conditions often occurred during the tuning of the discharge. After the discharge was tuned to a stable state with low reflected

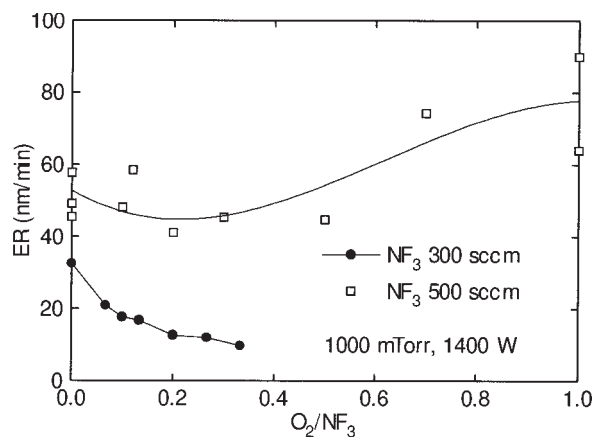


FIG. 4. The etch rate of silicon dioxide as a function of the flow ratio  $\text{O}_2/\text{NF}_3$ . The etch rate decreases as oxygen is added to a flow of 300 sccm of  $\text{NF}_3$ . If a higher  $\text{NF}_3$  flow is used (500 sccm), the etch rate remains on a constant level up to a ratio of 0.4, and then increases slightly upon further increase of the flow ratio.

power ( $<10$  W), the etch rates assumed regular values. Mass spectrometry measurements which were performed with an untuned discharge (200 W reflected power), showed a higher NO signal than a tuned discharge and the presence of  $\text{NF}_x$  ( $x=1,2$ ) species in the reaction chamber. It is likely that the high NO density is responsible for the fast  $\text{Si}_3\text{N}_4$  etch rate. The  $\text{SiO}_2$  etch rate is not influenced by the NO density. It is possible that  $\text{NF}_x$  species enhance the etching of  $\text{SiO}_2$  under these conditions.

## B. Optical emission and actinometry measurements

We performed actinometry measurements to monitor the production of atomic fluorine and oxygen in the discharge as a function of the flow  $\text{O}_2$  in  $\text{NF}_3$ . Actinometry with argon as a tracer gas has been widely used to determine the relative F atom density in  $\text{CF}_4/\text{O}_2$  and  $\text{SF}_6/\text{O}_2$  systems.<sup>12–15</sup> The method has been validated by Donnelly *et al.*<sup>16</sup> for the after-glow of  $\text{CF}_4/\text{O}_2$  and  $\text{NF}_3/\text{Ar}$  systems. The ground state density of a species  $X$  in the discharge,  $n_X$ , is proportional to the density of Ar and the ratio of the emission intensities<sup>17</sup>

$$n_X \propto n_{\text{Ar}}^* I_X / I_{\text{Ar}}, \quad (1)$$

where the Ar density is determined from the total gas density  $n_{\text{tot}}$  and the gas flows

$$n_{\text{Ar}} = n_{\text{tot}} = \frac{Q_{\text{Ar}}}{Q_{\text{NF}_3} + Q_{\text{O}_2} + Q_{\text{Ar}}}. \quad (2)$$

Typically, the intensity of the Ar  $4s'[1/2]^0 - 4p'[1/2]$  emission at 750.4 nm, whose upper level has an excitation energy of 13.48 eV, is set in relation with the F  $3s^2P - 3p^2P^0$  emission at 703.7 nm (14.76 eV), or the O  $3s^3S^0 - 3p^3P$  triplet at 844.6 nm (10.99 eV). In our experiments, however, the Ar (750.4 nm) line overlapped with other peaks, and the numerical determination of the intensity is very likely to have a systematic error. In order to eliminate this error, we included the Ar (763.5 nm,  $4s[1/2]^0 - 4p[1/2]^0$ )

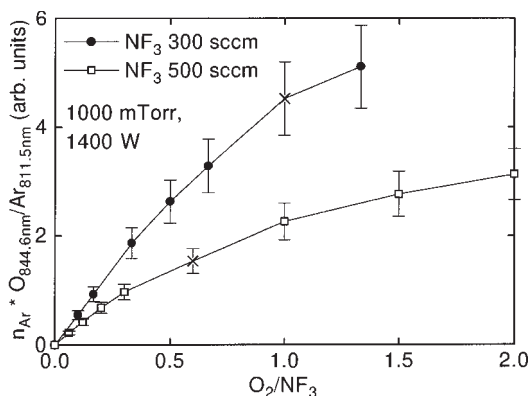


FIG. 5. The relative changes of the O atom concentration as determined by Ar actinometry. The flow of  $\text{NF}_3$  was kept constant at 300 and 500 sccm, respectively. As expected, the density of O atoms in the plasma region grows with the flow of oxygen. The production of atomic oxygen is higher by a factor of 1.9 for the low flow of  $\text{NF}_3$ .

$-4p[1\ 1/2])$  and Ar (811.5 nm,  $4s[1\ 1/2]^0 - 4p[2\ 1/2])$  lines into our analysis. The energies of the upper levels of these emissions, 13.17 and 13.08 eV, are very close to that of the Ar (750.4 nm) line. The determination of the emission intensities of these two emissions is straightforward, since no overlap with other emission lines occurs. In all our experiments, we find that the F/Ar (763.5 nm) and F/Ar (811.5 nm) ratios have the exact same dependency on the  $\text{O}_2$  flow. We decided to use the Ar emission at 811.5 nm as actinometer for all graphs shown here. As discussed recently by Petrovic *et al.*<sup>18</sup> and by Malyshev and Donnelly,<sup>19</sup> cascading from metastable states into the  $4p[2\ 1/2]$  level may contribute significantly to the Ar 811.5 nm emission, whereas the contribution to the Ar 750.5 nm emission is negligible. All changes in the plasma affecting the Ar metastable density will also affect the emission intensity of the Ar 811.5 nm line. This effect is not taken into account in our analysis. However, we estimate the error introduced by using the Ar 811.5 nm line to be 15% or less. This estimate is based on a comparison of Ar 750.4 and 811.5 nm emission intensities from a  $\text{CF}_4/\text{O}_2/\text{Ar}$  microwave plasma ignited in the same applicator under similar conditions. The Ar emission lines from this gas mixture are free of overlap. The normalized Ar 750.4 and 811.5 nm emission intensities, as a function of  $\text{O}_2$  flow, vary by a maximum of 15% in the  $\text{CF}_4/\text{O}_2/\text{Ar}$  system. This is reflected by the error bars in Fig. 5. Furthermore, the Ar 811.5 nm emission deviates from the dilution curve no more than 10% and in a nonsystematic way, which supports the notion that the metastable contribution does not depend on the  $\text{O}_2$  flow.

Walkup *et al.*<sup>20</sup> have compared Ar actinometry of O in  $\text{CF}_4/\text{O}_2$  discharges with two photon laser induced fluorescence measurements. They found that the O  $3s^3S^0 - 3p^3P$  triplet at 844.6 nm yields more reliable results for the ground state O atom density than the  $3s^5S^0 - 3p^5P$  triplet at 777 nm, since dissociative recombination of  $\text{O}_2^+$  molecules can significantly contribute to the population of the  $3p^5P$  level and the emission at 777 nm.

In Fig. 5, the relative change of the O atom concentration

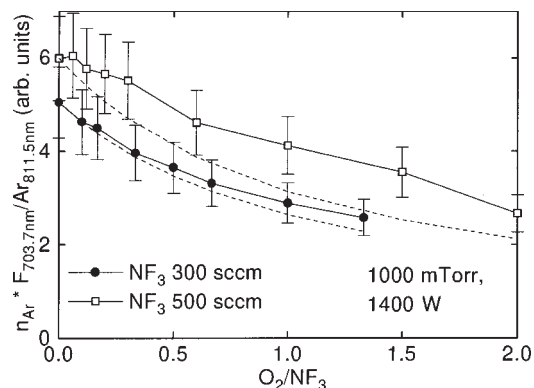


FIG. 6. The relative changes of the F atom concentration as determined by Ar actinometry. The same experimental parameters were used as in Fig. 5. The dashed lines indicate the calculated density of F under the assumption that dilution is the only effect of  $\text{O}_2$  addition to  $\text{NF}_3$ . At both flows of  $\text{NF}_3$ , the production of F atoms is not enhanced significantly. The F concentration decreases due to dilution. This is in contrast to  $\text{CF}_4/\text{O}_2$  microwave plasmas, and also to  $\text{NF}_3/\text{O}_2$  low density plasmas.

in the discharge region is shown as a function of the ratio  $\text{O}_2/\text{NF}_3$ . As one expects, the density of O atoms increases with the flow of  $\text{O}_2$ . However, in the case of 300 sccm of  $\text{NF}_3$ , the O atom concentration grows faster than in the case of 500 sccm of  $\text{NF}_3$ . The initial slopes of the curves differ by a factor of 1.9. At a fixed flow of 300 sccm of  $\text{O}_2$  (designated by crosses in Fig. 5), the density of ground state oxygen atoms is higher by a factor of 2.9 for the low flow of  $\text{NF}_3$ .

Figure 6 shows the behavior of the F atom concentration in the plasma as a function of oxygen addition. The dashed lines show the predicted F density under the assumption that dilution of gas phase species is the only effect on the production of F as  $\text{O}_2$  is added to the discharge. The concentration of F decreases with the addition of  $\text{O}_2$ . However, Fig. 6 indicates that the decrease of the F density for the case of 500 sccm of  $\text{NF}_3$  is less than predicted by the dilution effect by a margin significantly greater than the error. This indicates that the production rate of F atoms is slightly increased by the presence of oxygen in the discharge, but the total density decreases due to dilution.

In order to gain information about the chemical effects of the  $\text{O}_2$  in the discharge, relative changes of the emission intensities from  $\text{N}_2$  and NF were determined. Oxygen atoms can be expected to quickly oxidize the lower fluorides of  $\text{NF}_x$ ,<sup>21,22</sup> leading to a reduced density of  $\text{NF}_x$  ( $x=1,2$ ) in the plasma. The production of  $\text{N}_2$  is likely to decrease in favor of the generation of oxides of nitrogen.<sup>22</sup> The  $b\ 1^1\Sigma^+ - X\ 3^3\Sigma^-$  system of NF at 528.8 nm and the  $C\ 3^3\Pi_u - B\ 3^3\Pi_g$  system of  $\text{N}_2$  at 357.7 nm could be detected. The emission intensity of both  $\text{N}_2$  and NF in the plasma decreases more strongly than just due to the dilution effect (see Fig. 7), and the emission from NF vanishes at  $\text{O}_2/\text{NF}_3=2$ . This indicates the presence of chemical reactions of those species with O or  $\text{O}_2$ .

Optical emission from other species, e.g.,  $\text{F}_2$ , N, NO, or  $\text{NO}_2$ , could not be identified in the present work. This is consistent with the observation of other researchers for NF.<sup>23</sup>



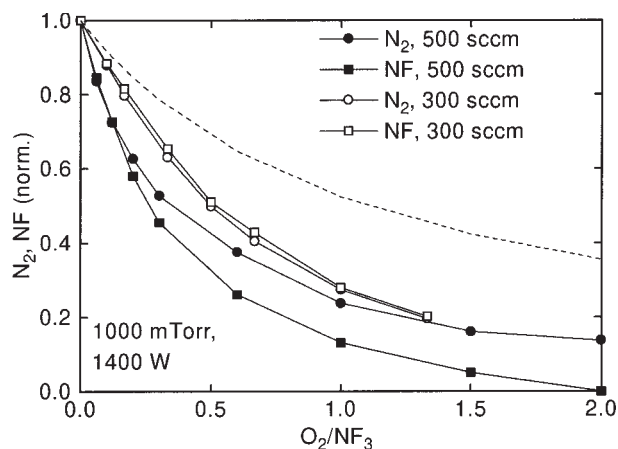


FIG. 7. The relative changes of the N<sub>2</sub> and NF emission intensities from the NF<sub>3</sub>/O<sub>2</sub> discharge. The same experimental parameters were used as in Fig. 5. Again, the dashed line indicates the dilution by O<sub>2</sub>. At both flows of NF<sub>3</sub>, the density of both species is reduced more than just by dilution alone.

and NF<sub>3</sub>/Ar<sup>16</sup> discharges. Atomic nitrogen and F<sub>2</sub> are suppressed by fast reactions with NF<sub>x</sub> species<sup>16</sup>



therefore their emission intensity is below the detection limit of our spectrograph. So far, no explanation for the absence of emission from NO can be given.

### C. Mass spectrometry measurements

We previously applied mass spectrometry to determine the relative changes in the concentration of reactive species in chemical dry etching.<sup>7</sup> As in our previous work, we measured the intensities of the species with and without a discharge ignited. The data is then plotted as the difference between the plasma-on and the plasma-off state, which represents the production and dissociation of species in the plasma better than the approach where the plasma-on state only is measured.

An analog spectrum of the afterglow of a microwave discharge in pure NF<sub>3</sub> is shown in panel (a) of Fig. 8, together with the spectrum obtained for no discharge ignited. This spectrum shows the NF<sub>3</sub> peak at mass number 71 and the cracking products NF and NF<sub>2</sub>. Background signals of O<sub>2</sub> and N<sub>2</sub> are also visible. These peaks disappear completely, as a discharge is ignited with 1400 W of microwave power. Instead, F, F<sub>2</sub>, and N<sub>2</sub> are produced. SiF<sub>3</sub> at 85 amu appears as a cracking product of SiF<sub>4</sub>, the product of etching reactions of quartz windows in the reactor. The difference spectrum  $I_{\text{PlasmaOn}} - I_{\text{PlasmaOff}}$  is shown in panel (b). The dissociation of species, like NF<sub>x</sub>, is represented as a negative peak. Generation of species, like N<sub>2</sub>, F<sub>2</sub>, and the F radical leads to positive peaks in the difference spectrum. Panel (c) of Fig. 8 shows the difference spectrum obtained from a NF<sub>3</sub>/O<sub>2</sub> mixture. Nitric oxide is produced in the discharge, and oxygen is visible as a negative peak.

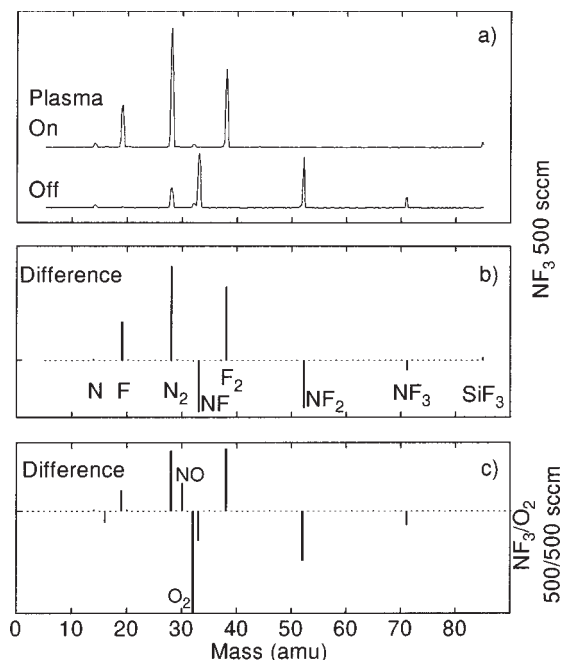


FIG. 8. Typical mass spectra sampled from the downstream reactive chamber. For the top panel pure NF<sub>3</sub> is used. The top panel shows analog spectra for no discharge and for the microwave discharge ignited, together with the difference spectrum. The NF<sub>x</sub> ( $x=1,2,3$ ) peaks disappear completely as the discharge is ignited. Therefore they appear as negative peaks in the difference spectrum. N<sub>2</sub>, F<sub>2</sub>, and F radicals are the main products of the NF<sub>3</sub> discharge. The bottom panel contains the difference spectrum of a NF<sub>3</sub>/O<sub>2</sub> mixture showing NO production.

tensity of the peak at 19 amu as a function of O<sub>2</sub> addition to 500 sccm of NF<sub>3</sub>. The density of F<sub>2</sub> decreases with increasing flow of O<sub>2</sub>. The dashed line in Fig. 9 is the dilution curve. The peak at 19 amu is due to atomic fluorine and electron impact dissociation of F<sub>2</sub> in the ionization region of the mass spectrometer. The data shown are not corrected for this effect, since an estimate for the F<sub>2</sub> contribution was not available.

It is known from previous work<sup>7</sup> that the etch rate of Si<sub>3</sub>N<sub>4</sub> is proportional to the density of NO in the reaction chamber. Figure 10 shows the normalized NO density down-

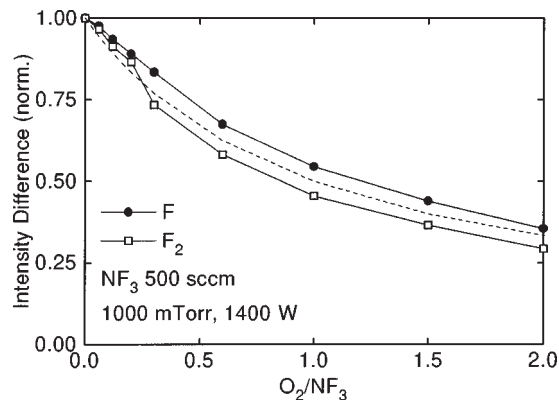


FIG. 9. The intensity difference between the plasma-on and plasma-off values,  $I_{\text{PlasmaOn}} - I_{\text{PlasmaOff}}$ , for the <sup>19</sup>F and the <sup>38</sup>F<sub>2</sub> peaks. Both difference values decrease as the flow of O<sub>2</sub> in NF<sub>3</sub> is increased from a ratio O<sub>2</sub>/NF<sub>3</sub> = 0 to O<sub>2</sub>/NF<sub>3</sub> = 2.

# Explore Litigation Insights

Docket Alarm provides insights to develop a more informed litigation strategy and the peace of mind of knowing you're on top of things.

## Real-Time Litigation Alerts



Keep your litigation team up-to-date with **real-time alerts** and advanced team management tools built for the enterprise, all while greatly reducing PACER spend.

Our comprehensive service means we can handle Federal, State, and Administrative courts across the country.

## Advanced Docket Research



With over 230 million records, Docket Alarm's cloud-native docket research platform finds what other services can't. Coverage includes Federal, State, plus PTAB, TTAB, ITC and NLRB decisions, all in one place.

Identify arguments that have been successful in the past with full text, pinpoint searching. Link to case law cited within any court document via Fastcase.

## Analytics At Your Fingertips



Learn what happened the last time a particular judge, opposing counsel or company faced cases similar to yours.

Advanced out-of-the-box PTAB and TTAB analytics are always at your fingertips.

## API

Docket Alarm offers a powerful API (application programming interface) to developers that want to integrate case filings into their apps.

## LAW FIRMS

Build custom dashboards for your attorneys and clients with live data direct from the court.

Automate many repetitive legal tasks like conflict checks, document management, and marketing.

## FINANCIAL INSTITUTIONS

Litigation and bankruptcy checks for companies and debtors.

## E-DISCOVERY AND LEGAL VENDORS

Sync your system to PACER to automate legal marketing.